Victor Iliev Rizov[1], Holm Altenbach[2]

ON THE ANALYSIS OF LENGTHWISE FRACTURE OF FUNCTIONALLY GRADED ROUND BARS

ANALIZA PODUŽNOG LOMA OKRUGLIH ŠTAPOVA OD FUNKCIONALNOG KOMPOZITA

Originalni naučni rad / Original scientific paper
UDK /UDC: 66.017/.018:539.42
Rad primljen / Paper received: 18.03.2019

Adresa autora / Author's address:
[1)] University of Architecture, Civil Engineering and Geodesy, Department of Technical Mechanics, Sofia, Bulgaria, email: v_rizov_fhe@uacg.bg
[2)] Lehrstuhl für Technische Mechanik und Geschäfts-führender Leiter Institut für Mechanik, Fakultät für Maschinenbau, Otto-von-Guericke-Universität Magdeburg, Deutschland, email: holm.altenbach@ovgu.de

Keywords
- functionally graded material
- lengthwise fracture
- round bar
- linear elastic behaviour

Ključne reči
- funkcionalni kompozitni materijal
- podužni lom
- okrugli štap
- linearno elastično ponašanje

Abstract

The strain energy release rate for lengthwise circular cylindrical cracks in round bars which are functionally graded in radial direction is derived by applying linear elastic fracture mechanics. The solution obtained is valid for a crack located arbitrarily in the radial direction of the bar cross-section. Besides, the modulus of elasticity and the shear modulus can be distributed arbitrarily in the radial direction. The functionally graded bars are loaded by axial forces, bending and torsion moments. The derived solution is applied to analyse the strain energy release rate for a lengthwise crack in a clamped functionally graded bar configuration. The external load of the clamped bar consists of an axial force and a torsion moment applied at the free end of the internal crack arm and a bending moment applied at the free end of the bar. In order to verify the solution, the strain energy release rate in the clamped bar is determined also by considering the balance of energy and by applying the compliance method. The influence of various factors such as crack location in the radial direction, the material gradient and loading conditions on strain energy release rate in the clamped bar configuration are investigated and discussed.

Izvod

Primenom linearno elastične mehanike loma, izvedena je brzina oslobađanja deformacione energije kod podužnih kružnih cilindričnih prslina u okruglim štapovima od funkcionalnog kompozitnog materijala sa slojevima u radijalnom pravcu. Dobijeno rešenje važi za prslinu proizvoljno lociranu u radijalnom pravcu preseka štapa. Osim toga, modul elastičnosti i modul klizanja su takođe proizvoljni u radijalnom pravcu. Štapovi od funkcionalnog kompozita su opterećeni aksijalnim silama i momentima savijanja i torzije. Izvedeno rešenje je primenjeno u analizi brzine oslobađanja deformacione energije podužne prsline kod uklještenog štapa od funkcionalnog kompozita. Spoljašnja opterećenja uklještenog štapa su aksijalna sila i moment uvijanja, koji deluju na slobodnom kraju kraka unutrašnje prsline, i moment savijanja, koji deluje na slobodnom kraju štapa. Radi provere rešenja, brzina oslobađanja energije deformacije uklještenog štapa se određuje razmatranjem ravnoteže energije i primenom metode popustljivosti. Razmotreni su i diskutovani uticaji pojedinih faktora, kao što su lokacija prsline u radijalnom pravcu, gradijent materijala i uslovi opterećenja na brzinu oslobađanja deformacione energije kod uklještenog štapa.

INTRODUCTION

Functionally graded materials are inhomogeneous composites of two or more constituent materials. The most important feature of functionally graded materials is the smooth variation of their properties along one or more directions in the solid, /1-7/. Variation of material properties can be tailored in order to improve the performance of functionally graded structural members and components to externally applied loads. In recent years, functionally graded materials have been frequently used as advanced structural materials in various engineering applications in aerospace, nuclear reactors, airplane industry and bioengineering.

Accessing of structural integrity, reliability and safety of functionally graded structural members and components is closely related with their fracture behaviour. Therefore, crack problems of functionally graded materials are an important subject of research that continues to attract the attention of academic community around the globe /8-12/.

Basic problems of fracture mechanics of functionally graded materials have been discussed in /8/. Methods for solving different crack problems in functionally graded materials have been developed. The fracture analyses performed and the results obtained can be useful for material scientists and design engineers which work in the field of functionally graded materials.

Various studies of fracture in functionally graded composite materials have been reviewed in /9/. Analyses of cracks oriented parallel or perpendicular to the direction of material gradient have been considered. Solutions for nonstraight cracks have also been discussed. Investigations of fracture behaviour of functionally graded materials under static and cyclic fatigue crack loading conditions by applying linear elastic fracture mechanics have been summarized.

An engineering method for predicting the strength of functionally graded structural members containing cracks has been developed in /10/. The method has been applied to a functionally graded linear elastic beam subjected to three-point bending. The beam under consideration has a rectangular cross-section and is functionally graded in the thickness direction. A functionally graded linear elastic plate loaded in tension has also been analyzed.

The present paper is focused on deriving a solution to the strain energy release rate for a lengthwise circular cylindrical crack in functionally graded round bars exposed to external mechanical loading which induces axial forces and bending and torsion moments. It is assumed that the bars are functionally graded in radial direction. A solution to the strain energy release rate is obtained for arbitrary variation of the modulus of elasticity and the shear modulus within the radial coordinate. The solution obtained can be used for a cylindrical crack located arbitrary in radial direction. The solution is applied to analyse the strain energy release rate for a lengthwise cylindrical crack in a clamped functionally graded round bar. The strain energy release rate in the clamped bar is determined also by considering the balance of energy for verification. A further verification is performed by applying the compliance method. The influence of loading conditions, material properties and crack location on the strain energy release rate in the clamped bar is investigated and discussed.

SOLUTION PROCEDURE TO THE STRAIN ENERGY RELEASE RATE

In order to derive the strain energy release rate, a portion of a functionally graded round bar containing the crack front is considered (Fig. 1).

The bar cross-section is a circle of radius r_2. The axial force and torsion and bending moments in the bar cross-section ahead of the crack front are denoted by N_3, T_3 and M_3, respectively (Fig. 1). The lengthwise crack is a circular cylindrical surface of radius r_1. Thus, the crack front is a circle of radius r_1. In the present analysis, the internal crack arm is treated as a round bar of radius r_1. The external crack arm is treated as a bar of ring-shaped cross-section of internal radius r_1, and external radius r_2.

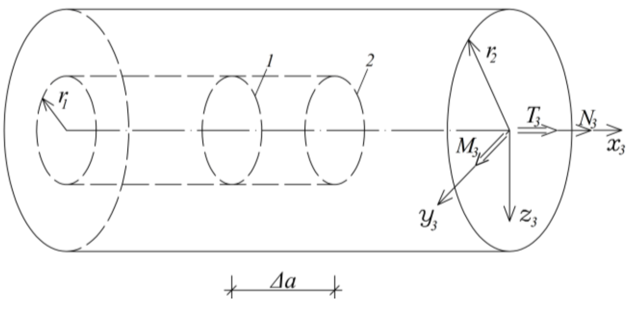

Figure 1. Portion of a round bar with the crack front position (1-before increase of lengthwise crack, 2-after increase of the lengthwise crack).

According to linear elastic fracture mechanics, the strain energy release rate, G, for the crack problem in Fig. 1 is given as

$$G=-\frac{\Delta U}{l_{cf}\,\Delta a}\,, \tag{1}$$

where: ΔU is the change of strain energy; l_{cf} is the length of crack front; Δa is a small increase in crack length. The change of strain energy due to the increase of crack length is expressed as

$$\Delta U=\Delta a\int_0^{r_1}\int_0^{2\pi}u_{01}rdrd\phi+\Delta a\int_{r_1}^{r_2}\int_0^{2\pi}u_{02}rdrd\phi-\Delta a\int_0^{r_2}\int_0^{2\pi}u_{03}rd\,rd\phi \tag{2}$$

where the first and second terms in the right-hand side of the equation are the strain energies stored-up in portions of length Δa, in the two crack arms behind the crack front; the third term is the strain energy in the uncracked bar portion of length Δa, ahead of the crack front; u_{01}, u_{02} and u_{03} are, respectively, strain energy densities in internal and external crack arms and in the uncracked bar portion ahead of the crack front.

The length of crack front is calculated as

$$l_{cf}=2\pi r_1\,. \tag{3}$$

By substituting Eqs.(2) and (3) in Eq.(1), the strain energy release rate is expressed as

$$G=\frac{1}{2\pi r_1}\left(\int_0^{r_1}\int_0^{2\pi}u_{01}rdrd\phi+\int_{r_1}^{r_2}\int_0^{2\pi}u_{02}rdrd\phi-\int_0^{r_2}\int_0^{2\pi}u_{03}rdrd\phi\right). \tag{4}$$

The strain energy density in the internal crack arm is written as

$$u_{01}=u_{01\sigma}+u_{01\tau}\,, \tag{5}$$

where: $u_{01\sigma}$ and $u_{01\tau}$ are the densities of strain energy due to the axial force and bending moment and of the torsion moment, in respect. The strain energy density due to axial force and bending moment is written as

$$u_{01\sigma}=\frac{1}{2}\sigma\varepsilon\,, \tag{6}$$

where: σ is the normal stress; ε is the strain. The normal stresses are obtained by Hooke's law

$$\sigma=E\varepsilon\,, \tag{7}$$

where: the modulus of elasticity varies continuously in the radial direction,

$$E=E(r)\,. \tag{8}$$

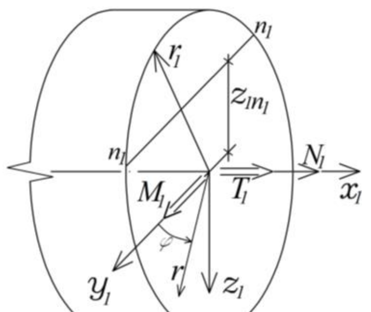

Figure 2. Cross-section of the internal crack arm behind the crack front (position of neutral axis is marked by n_1–n_1).

According to Bernoulli's hypothesis for plane sections, ε is distributed linearly along the thickness of the internal crack arm

$$\varepsilon = \kappa_1 (z_1 - z_{1n_1}) , \tag{9}$$

where

$$-r_1 \le z_1 \le r_1 . \tag{10}$$

It should be noted that Bernoulli's hypothesis is applicable since bars of a high length to thickness ratio are under consideration in the present paper. In Eq.(9), κ_1 is the curvature of the internal crack arm, z_{1n1} is the coordinate of the neutral axis (Fig. 2).

It is obvious that the neutral axis shifts from the centroid since the internal crack arm is loaded by bending moment and axial force. By substituting Eqs.(7) and (9) in Eq,(6), one arrives at

$$u_{01\sigma} = \frac{1}{2} E \left[\kappa_1 (z_1 - z_{1n_1}) \right]^2 , \tag{11}$$

where: E is a function of the radial coordinate.

The curvature and the neutral axis coordinate are determined by using the following equations for equilibrium of the cross-section of internal crack arm:

$$N_1 = \iint_{A_1} \sigma dA , \tag{12}$$

$$M_1 = \iint_{A_1} \sigma z_1 dA , \tag{13}$$

where: A_1 is the area of the internal crack arm cross-section; N_1 and M_1 are, respectively, the axial force and the bending moment in the cross-section of the internal crack arm behind the crack front. By using the designations in Fig. 2, Eqs.(12) and (13) are expressed in polar coordinates as

$$N_1 = \int_0^{r_1} \int_0^{2\pi} \sigma r dr d\varphi , \tag{14}$$

$$M_1 = \int_0^{r_1} \int_0^{2\pi} \sigma r^2 \sin\varphi dr d\varphi , \tag{15}$$

where: σ is obtained by Eq.(7). In order to facilitate the integration in Eqs.(14) and (15), the distribution of lengthwise strains, Eq.(9), is rewritten as

$$\varepsilon = \kappa_1 (r \sin\varphi - z_{1n_1}) , \tag{16}$$

where: the polar angle, φ, is defined in Fig. 2.

However, there are three unknowns: κ_1, z_{1n1} and M_1, in Eqs.(14) and (15). Therefore, two other equations are worked-out by considering the equilibrium of the cross-section of external crack arm behind the crack front

$$N_2 = \int_{r_1}^{r_2} \int_0^{2\pi} \sigma_g r dr d\phi , \tag{17}$$

$$M_2 = \int_{r_1}^{r_2} \int_0^{2\pi} \sigma_g r^2 \sin\phi dr d\phi , \tag{18}$$

where: N_2 and M_2 are, respectively, the axial force and the bending moment in the cross-section of external crack arm behind the crack front. The normal stress in the external crack arm, σ_g, is obtained by the Hooke's law

$$\sigma_g = E \varepsilon_g , \tag{19}$$

where: lengthwise strain, ε_g, is distributed linearly along the height of the external crack arm cross-section,

$$\varepsilon_g = \kappa_2 (r \sin\varphi - z_{2n_2}) . \tag{20}$$

In Eq.(20), κ_2 and z_{2n2} are the curvature and the coordinate on neutral axis, respectively. Since the axial force and the bending moment generate mode II crack loading conditions, the curvature of external crack arm is the same as the curvature of internal crack arm,

$$\kappa_2 = \kappa_1 . \tag{21}$$

Also, it is obvious that

$$M_1 + M_2 = M , \tag{22}$$

where: M is the bending moment in the bar cross-section behind the crack front. Thus, the bending moment in the external crack arm is expressed as

$$M_2 = M - M_1 . \tag{23}$$

Equations (14), (15), (17), (18), (21) and (23) can be solved with respect to κ_1, z_{1n1}, κ_2, z_{2n2}, M_1 and M_2 for arbitrary continuous variation of the modulus of elasticity with the radial coordinate. After that, κ_1 and z_{1n1} are substituted in Eq.(11) to calculate $u_{01\sigma}$.

The strain energy density due to the torsion of internal crack arm is written as

$$u_{01\tau} = \frac{1}{2} \tau \gamma , \tag{24}$$

where: τ and γ are the shear stress and strain, respectively. The shear stress is obtained by applying the Hooke's law

$$\tau = S \gamma , \tag{25}$$

where the shear modulus, S, varies arbitrary with the radial coordinate

$$S = S(r) . \tag{26}$$

Since we assume validity of the Bernoulli's hypothesis, the shear strains are distributed linearly along the radius

$$\gamma = r \frac{\gamma_d}{r_1} , \tag{27}$$

where:

$$0 \le r \le r_1 . \tag{28}$$

In Eq.(27), γ_d is the shear strain at the periphery of the internal crack arm. The following equation for equilibrium of the internal crack arm cross-section is used to determine γ_d,

$$T_1 = \iint_{A_1} \tau r dA , \tag{29}$$

where: T_1 is the torsion moment in the internal crack arm cross-section behind the crack front. Equation (29) is expressed in polar coordinates as

$$T_1 = \int_0^{r_1} \int_0^{2\pi} \tau r^2 dr d\varphi , \tag{30}$$

where: τ is obtained by Eq.(25). Equation (30) can be used to determine γ_d for arbitrary continuous variation of the shear modulus with the radial coordinate.

By substituting Eqs.(25) and (27) in Eq.(24), one arrives at

$$u_{01\tau} = \frac{1}{2} S \left(\gamma_d \frac{r}{r_1} \right)^2 , \tag{31}$$

where: S is a continuous function of the radial coordinate; γ_d is obtained from Eq.(30).

The final expression for strain energy density in the internal crack arm cross-section behind the crack front is obtained by substituting Eqs.(11) and (31) in Eq.(5).

Equation (5) is applied also to calculate the strain energy density in the external crack arm cross-section behind the crack front. For this purpose, z_{1n1} in Eq.(11) is replaced with z_{2n2}. Also, γ_d and r_1 in Eq.(31) are replaced with γ_g and r_2, respectively. The shear strain at the periphery of the external crack arm, γ_g, is determined from the following equilibrium equation of the external crack arm cross-section:

$$T_2 = \int_{r_1}^{r_2} \int_{0}^{2\pi} \tau_g r^2 dr d\varphi \,, \tag{32}$$

where: T_2 is the torsion moment in the external crack arm behind the crack front. The shear stress in the external crack arm, τ_g, is obtained by the Hooke's law

$$\tau_g = Sr\frac{\gamma_g}{r_2} \,. \tag{33}$$

The strain energy density in the bar cross-section ahead of the crack front is obtained by Eq.(5). For this purpose, κ_1 and z_{1n1} in Eq.(11) are replaced with κ_3 and z_{3n3}, respectively (κ_3 and z_{3n3} are the curvature and the coordinate of neutral axis in the bar cross-section ahead of the crack front). Equations (14) and (15) are used to determine κ_3 and z_{3n3}. For this purpose, N_1, M_1, r_1 and σ are replaced with N_3, M_3, r_2 and σ_n, respectively. It is obvious that

$$N_3 = N_1 + N_2 \,, \tag{34}$$

$$M_3 = M_1 + M_2 \,. \tag{35}$$

The normal stress, σ_n, in the bar cross-section ahead of the crack front is found by Hooke's law Eq.(7). The lengthwise strain is found by replacing κ_1 and z_{1n1} in Eq.(9) with κ_3 and z_{3n3}, respectively. In Eq.(31), γ_d and r_1 are replaced with γ_n and r_2. The shear strain, γ_n, at the periphery of the bar is determined by using Eq.(30). For this purpose, T_1, r_1 and τ are replaced with T_3, r_2 and τ_n, respectively. Obviously,

$$T_3 = T_1 + T_2 \,. \tag{36}$$

The shear stress, τ_n, is expressed by Hooke's law Eq.(25). The shear strain is obtained by replacing γ_d and r_1 in Eq.(27) with γ_n and r_2, respectively.

The strain energy release rate is calculated by substituting strain energy densities in Eq.(4). It should be mentioned that the solution to strain energy release rate derived in the present paper can be applied for functionally graded round bar configurations with arbitrary variation of modulus of elasticity and shear modulus with the radial coordinate.

NUMERICAL EXAMPLE

In the present section of the paper, the strain energy release rate for a lengthwise circular cylindrical crack in a clamped functionally graded round bar is analysed by applying the solution obtained in the previous section.

The round bar under consideration is depicted in Fig. 3. There is a lengthwise crack of length a in the bar. The radius of bar cross-section is r_2. The internal crack arm has a circular cross-section of radius, r_1. The bar length is l. The bar is clamped at its right-hand end.

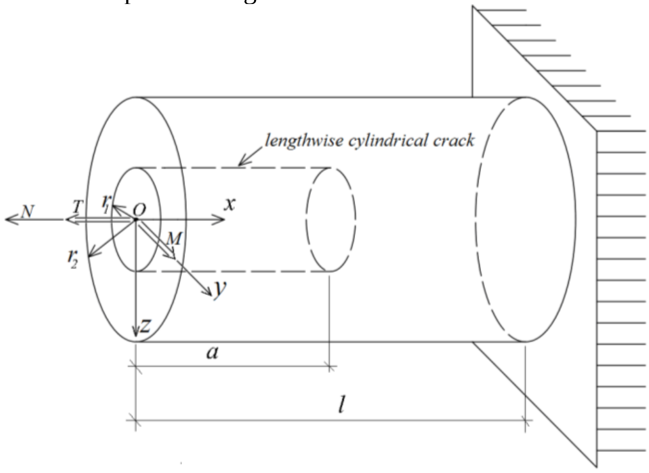

Figure 3. Geometry and loading of a clamped round bar with a lengthwise cylindrical crack.

External loading includes one bending moment, M, applied at the free end of the bar, one axial force, F, and one torsion moment, T, applied at the free end of internal crack arm. It is apparent that the internal crack arm is loaded by axial force and by torsion and bending moments, while the external crack arm is loaded in pure bending since M is distributed on both crack arms. The uncracked bar portion, $a \le x \le l$, is loaded by axial force and by torsion and bending moments. Therefore,

$$N_1 = F \,,\; T_1 = T \,, \tag{37}$$

$$N_2 = 0 \,,\; T_2 = 0 \,, \tag{38}$$

$$N_3 = F \,, T_3 = T \,. \tag{39}$$

The bending moments in the two crack arms, M_1 and M_2, are obtained from Eqs.(14), (15), (17), (18), (21) and (23).

For the functionally graded round bar shown in Fig. 3, it is assumed that the modulus of elasticity and the shear modulus vary continuously with the radial coordinate, according to the following power laws:

$$E = E_0 + (E_t - E_0)\left(\frac{r}{r_2}\right)^m \,, \tag{40}$$

$$S = S_0 + (S_t - S_0)\left(\frac{r}{r_2}\right)^p \,, \tag{41}$$

where: $$0 \le r \le r_2 \,. \tag{42}$$

In Eqs.(40) and (41), E_0 and S_0 are the values of modulus of elasticity and shear modulus at the centre of bar cross-section, respectively; E_t and S_t are values of the modulus of elasticity and shear modulus at the periphery of the bar, respectively. The material properties, m and p, govern the distribution of E and S in the radial direction, respectively.

In order to calculate the strain energy density in the internal crack arm cross-section behind the crack front, first, κ_1, z_{1n1}, κ_2, z_{2n2}, M_1 and M_2 are determined. For this purpose, by substituting Eq.(40) in Eqs.(14), (15), (17) and (18) and taking into account Eqs.(21) and (23), one obtains the following four equations with unknowns, κ_1, z_{1n1}, z_{2n2} and M_1:

$$N_1 = -E_0 z_{1n_1} r_1^2 \pi\kappa_1 + 2\eta z_{1n_1} \pi\kappa_1 \frac{r_1^{m+2}}{m+2}\,, \qquad (43)$$

$$M_1 = \frac{1}{4} E_0 \kappa_1 \pi r_1^4 + \eta\kappa_1 \pi \frac{r_1^{m+4}}{m+4}\,, \qquad (44)$$

$$N_2 = -E_0 z_{2n_2} (r_2^2 - r_1^2)\pi\kappa_1 + 2\eta z_{2n_2} \pi\kappa_1 \frac{r_2^{m+2} - r_1^{m+2}}{m+2}\,, \qquad (45)$$

$$M - M_1 = \frac{1}{4} E_0 \kappa_1 \pi (r_2^4 - r_1^4) + \eta\kappa_1 \pi \frac{r_2^{m+4} - r_1^{m+4}}{m+4}\,, \qquad (46)$$

where: $\eta = (E_t - E_0)/ r_2^m$. Equations (43)-(46) are solved with respect to κ_1, z_{1n1}, z_{2n2} and M_1 by using the MatLab computer program. Then, $u_{01\sigma}$ is derived by substituting Eq.(40), κ_1 and z_{1n1} in Eq.(11).

Further, by substituting Eqs.(25), (27) and (41) in (30), one arrives at

$$T_1 = \frac{1}{2} S_0 \gamma_d r_1^3 \pi + 2\theta\gamma_d \pi \frac{r_1^{p+3}}{p+4}\,, \qquad (47)$$

where: $\theta = (S_t - S_0)/ r_2^p$. From Eq.(47), one derives

$$\gamma_d = 2T_1(p+4)/[S_0 r_1^3 \pi(p+4) + 4\theta\pi r_1^{p+3}]\,. \qquad (48)$$

After that, $u_{01\tau}$ is determined by substituting Eq.(41) in Eq.(31). The strain energy density in the internal crack arm cross-section behind the crack front is found by substituting $u_{01\sigma}$ and $u_{01\tau}$ in Eq.(5).

The strain energy density in the cross-section of external crack arm behind the crack front is determined in the following way. First, z_1 and z_{1n1} are replaced, respectively, with z_2 and z_{2n2} in Eq.(11). Also, Eq.(40) is substituted in Eq.(11). Since the external crack arm is loaded in pure bending, $u_{02} = u_{02\sigma}$.

Equations (43) and (44) are used to determine κ_3 and z_{3n3}. For this purpose, after replacing N_1, M_1, r_1, κ_1 and z_{1n1} with N_3, M_3, r_2, κ_3 and z_{3n3}, Eqs.(43) and (44) are solved with respect to κ_3 and z_{3n3} by using the MatLab computer program. Then, $u_{03\sigma}$ is obtained by replacing z_1, z_{1n1} and κ_1 with z_3, z_{3n3} and κ_3 in Eq.(11). Equation (31) is applied to calculate $u_{03\tau}$. For this purpose, γ_d and $r_1$are replaced with γ_n and r_2, respectively. Equation (48) is used to determine γ_n. For this purpose, T_1, r_1 and γ_d are replaced, respectively, with T_3, r_2 and γ_n. The strain energy density in the bar cross-section ahead of the crack front is written as $u_{03} = u_{03\sigma} + u_{03\tau}$.

The strain energy release rate for the crack problem in Fig. 3 is derived by substituting u_{01}, u_{02} and u_{03} in Eq.(4). The result is

$$G = \frac{1}{2\pi R_1}(\omega_1 + \omega_2 + \omega_3 + \omega_4 + \omega_5)\,, \qquad (49)$$

where

$$\omega_1 = \frac{\kappa_1^2}{2}\left(\frac{1}{4}E_0 \pi r_1^4 + E_0 z_{1n_1}^2 \pi r_1^2 + \eta\pi \frac{r_1^{m+4}}{m+4} + 2\eta\pi z_{1n_1}^2 \frac{r_1^{m+2}}{m+2}\right),$$

$$\omega_2 = \pi\gamma_d^2 \left(\frac{1}{4} S_0 r_1^2 + \theta \frac{r_1^{p+2}}{p+4}\right),$$

$$\omega_3 = \frac{\kappa_2^2}{2}\left(\frac{1}{4}E_0 \pi (r_2^4 - r_1^4) + E_0 z_{2n_2}^2 \pi (r_2^2 - r_1^2) + \eta\pi \frac{r_2^{m+4} - r_1^{m+4}}{m+4} + 2\eta\pi z_{2n_2}^2 \frac{r_2^{m+2} - r_1^{m+2}}{m+2}\right),$$

$$\omega_4 = \frac{\kappa_3^2}{2}\left(\frac{1}{4}E_0 \pi r_2^4 + E_0 z_{3n_3}^2 \pi r_2^2 + \eta\pi \frac{r_2^{m+4}}{m+4} + 2\eta\pi z_{3n_3}^2 \frac{r_2^{m+2}}{m+2}\right),$$

$$\omega_5 = \pi\gamma_n^2 \left(\frac{1}{4} S_0 r_2^2 + \theta \frac{r_2^{p+2}}{p+4}\right).$$

In order to check Eq.(49), the strain energy release rate is obtained also by analysing the energy balance. For this purpose, a small increase of the crack length, Δa, is assumed. The energy balance is written as

$$F\delta u + M\delta\psi + T\delta\varphi = \frac{\partial U}{\partial a}\delta a + G l_{cf}\delta a\,, \qquad (50)$$

where: δu and $\delta\varphi$ are, respectively, increases in lengthwise displacement and angle of twist of the free end of the internal crack arm; $\delta\psi$ is the increase of the angle of rotation of free end of the bar; U is the strain energy cumulated in the bar. From Eq.(50), one obtains

$$G = \frac{F}{l_{cf}}\frac{\partial u}{\partial a} + \frac{M}{l_{cf}}\frac{\partial \psi}{\partial a} + \frac{T}{l_{cf}}\frac{\partial \varphi}{\partial a} - \frac{1}{l_{cf}}\frac{\partial U}{\partial a}\,. \qquad (51)$$

By substituting Eq.(3) in Eq.(51), one arrives at

$$G = \frac{1}{2\pi r_1}\left(F\frac{\partial u}{\partial a} + M\frac{\partial \psi}{\partial a} + T\frac{\partial \varphi}{\partial a} - \frac{\partial U}{\partial a}\right). \qquad (52)$$

The integrals of Maxwell-Mohr are used to determine u, ψ and φ. The result is

$$u = \varepsilon_\alpha a + \varepsilon_\beta (l - a)\,, \qquad (53)$$

$$\psi = \kappa_1 a + \kappa_3 (l - a)\,, \qquad (54)$$

$$\varphi = \frac{\gamma_d}{r_1} a + \frac{\gamma_n}{r_2}(l - a)\,. \qquad (55)$$

In Eq.(53), ε_α and ε_β are the lengthwise strains at the centres in cross-sections of internal crack arm and the uncracked beam portion, respectively. By substituting $z_1 = 0$ in Eq.(9), ε_α is written as

$$\varepsilon_\alpha = -\kappa_1 z_{1n_1}\,. \qquad (56)$$

Similarly, ε_β is obtained as

$$\varepsilon_\beta = -\kappa_3 z_{3n_3}\,. \qquad (57)$$

The strain energy cumulated in the bar is found by integrating strain energy densities in the volume of the internal and external crack arms and the uncracked bar portion

$$U = a\int_0^{r_1}\int_0^{2\pi} u_{01} r dr d\varphi + a\int_{r_1}^{r_2}\int_0^{2\pi} u_{02} r dr d\varphi + (l - a)\int_0^{r_2}\int_0^{2\pi} u_{03} r dr d\varphi\,. \qquad (58)$$

By substituting Eqs.(53)-(58) in Eq.(52), one derives the following expression for the strain energy release rate:

$$G = \frac{1}{2\pi r_1}\left[F(-\kappa_1 z_{1n_1} + \kappa_3 z_{3n_3}) + M(\kappa_1 - \kappa_3) + T\left(\frac{\gamma_d}{r_1} - \frac{\gamma_n}{r_2}\right) - \omega_1 - \omega_2 - \omega_3 + \omega_4 + \omega_5\right]. \qquad (59)$$

It should be noted that strain energy release rates calculated by Eq.(59) are exact match of these obtained by Eq.(49). This fact is a verification of strain energy release rate analyses developed in the present paper.

The compliance method is used also to verify the solution to the strain energy release rate Eq.(49). According to the compliance method, the strain energy release rate is written as

$$G=\frac{1}{2l_{cf}}\left(F^2\frac{dC_F}{da}+M^2\frac{dC_M}{da}+T^2\frac{dC_T}{da}\right), \qquad (60)$$

where the compliances of the bar are expressed as

$$C_F=\frac{u}{F},\ C_M=\frac{\psi}{M},\ C_T=\frac{\varphi}{T}. \qquad (61)$$

By substituting Eqs.(3), (53)-(55) in Eq.(60), one arrives at

$$G=\frac{1}{4\pi r_1}\left[F(-\kappa_1 z_{1n_1}+\kappa_3 z_{3n_3})+M(\kappa_1-\kappa_3)+T\left(\frac{\gamma_d}{r_1}-\frac{\gamma_n}{r_2}\right)\right]. \qquad (62)$$

Strain energy release rates obtained by Eq.(62) match exactly these calculated by Eq.(49) which is also a verification of the analysis developed in the present paper.

Parametric investigations are performed in order to evaluate the influence of crack location in radial direction, material properties and loading conditions on strain energy release rate for the crack problem shown in Fig. 3. For this purpose, calculations of strain energy release rate are carried out by Eq.(49). The results obtained are presented in non-dimensional form by using the formula $G_N = G/(E_0 r_2)$. It is assumed that $l = 0.2$ m, $r_2 = 0.003$ m, $F = 500$ N, $M = 20$ Nm and $T = 30$ Nm.

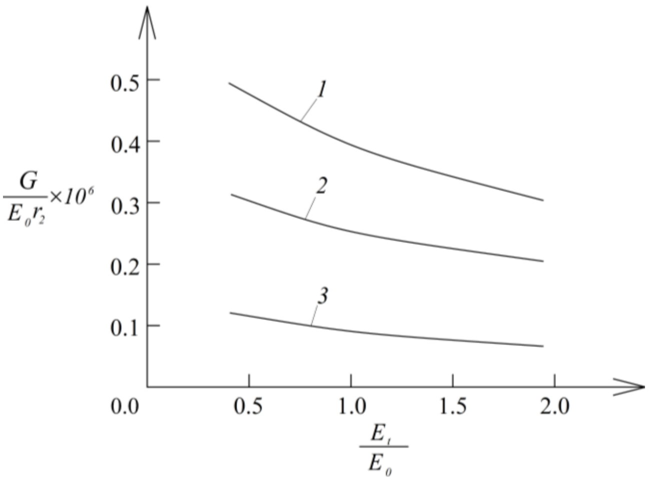

Figure 4. Strain energy release rate in non-dimensional form plotted against E_t/E_0 ratio (curve 1 at $r_1/r_2 = 0.25$; curve 2 at $r_1/r_2 = 0.50$; and curve 3 at $r_1/r_2 = 0.75$).

The effect of crack location in the radial direction on strain energy release rate is analysed. For this purpose, r_1/r_2 ratio which characterizes the crack location in the radial direction is introduced. The strain energy release rate is calculated at three r_1/r_2 ratios. The results obtained are illustrated in Fig. 4 where the strain energy release rate in non-dimensional form is plotted against E_t/E_0 ratio at three r_1/r_2 ratios for $S_0/E_0 = 0.8$, $S_t/S_0 = 0.7$, $m = 0.4$ and $p = 0.5$. The curves in Fig. 4 indicate that the strain energy release rate decreases with increasing of r_1/r_2 ratio. Figure 4 shows also that increase of E_t/E_0 ratio leads to decrease in the strain energy release rate. This finding is attributed to the increase of the bar stiffness.

The influence of S_0/E_0 ratio and material property m, on strain energy release rate in the functionally graded bar shown in Fig. 3 is evaluated. For this purpose, calculations of strain energy release rate are performed at various S_0/E_0 ratios for three values of m. The strain energy release rate is plotted in non-dimensional form against S_0/E_0 ratio at $r_1/r_2 = 0.25$ in Fig. 5. One can observe in Fig. 5 that the strain energy release rate decreases with increasing of S_0/E_0 ratio. Increase of m also leads to decrease of the strain energy release rate.

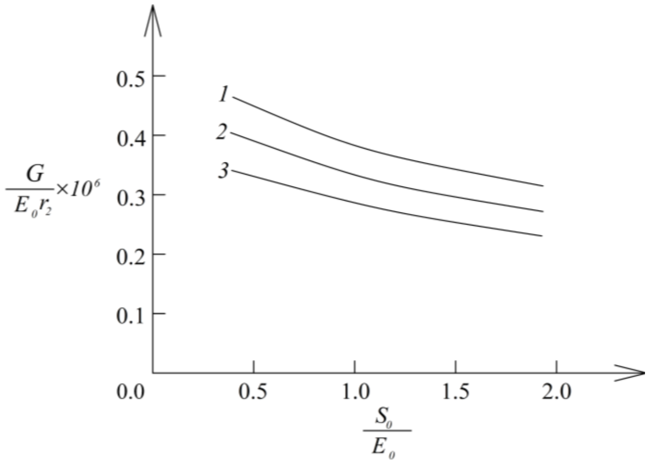

Figure 5. Strain energy release rate in non-dimensional form plotted against S_0/E_0 ratio (curve 1 at $m = 0.5$; curve 2 at $m = 0.7$; and curve 3 at $m = 0.9$).

The effect of material property p, and S_t/S_0 ratio on the strain energy release rate is elucidated in Fig. 6 where the strain energy release rate in non-dimensional form is plotted against S_t/S_0 ratio at three values of p for $r_1/r_2 = 0.25$. It can be observed that the strain energy release rate decreases with increasing of S_t/S_0 ratio (Fig. 6). The strain energy release rate decreases also with increasing of p.

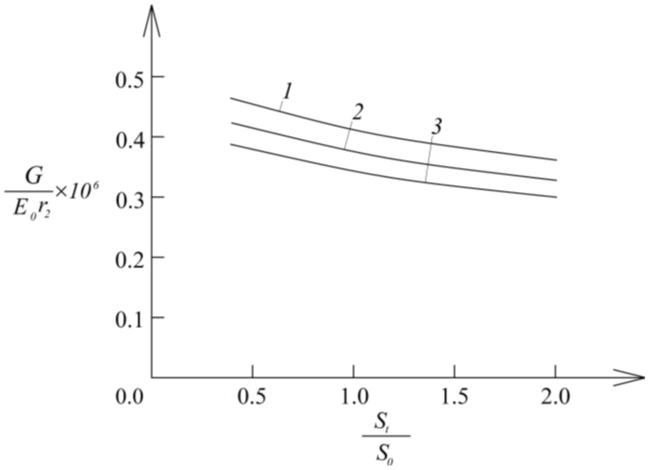

Figure 6. Strain energy release rate in non-dimensional form plotted against S_t/S_0 ratio (curve 1 at $p = 0.4$, curve 2 at $p = 0.6$ and curve 3 at $p = 0.8$).

The influence of loading conditions on the strain energy release rate is investigated too. For this purpose, the strain energy release rate in non-dimensional form is plotted against *T/F* ratio at three *T/M* ratios in Fig. 7 for $r_1/r_2 = 0.25$. Figure 7 shows that the strain energy release rate increases with increasing of both *T/F* and *T/M* ratios.

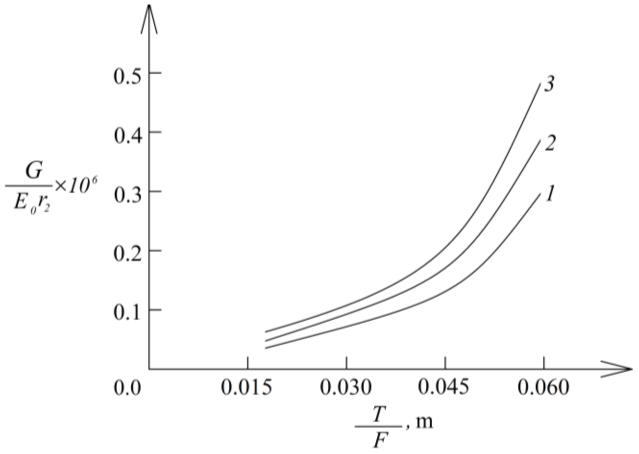

Figure 7. Strain energy release rate in non-dimensional form plotted against *T/F* ratio (curve 1 at *T/M* = 0.5; curve 2 at *T/M* = 1.0 and curve 3 at *T/M* = 1.5).

CONCLUSIONS

A solution procedure to the strain energy release rate for lengthwise cracks in functionally graded round bars is developed by applying methods of linear elastic fracture mechanics. The bars are loaded by axial forces and bending and torsion moments. The lengthwise cracks under consideration are circular cylindrical surfaces. The internal crack arm is treated as a bar of circular cross-section. The external crack arm is treated as a bar of ring-shaped cross-section. A solution to the strain energy release rate is derived assuming that the crack is located arbitrarily in radial direction. The solution holds for bars which are functionally graded in the radial direction (modulus of elasticity and shear modulus vary continuously in the radial direction).

The solution is applied to analyse the strain energy release rate for a lengthwise cylindrical crack in a clamped functionally graded round bar. Power laws are used to describe the distribution of the modulus of elasticity and the shear modulus in radial direction. The bar is loaded by an axial force and a torsion moment applied at the free end of the internal crack arm and a bending moment applied at the free end of the bar. The strain energy release rate in the clamped functionally graded round bar is derived also by considering the energy balance and by applying the compliance method for verification. Effects of the crack location in the radial direction, material gradients and the loading conditions on strain energy release rate are elucidated. It is found that the strain energy release rate decreases with increasing of the radius of internal crack arm cross-section. Material gradients in the radial direction are characterized by E_t/E_0 and S_t/S_0 ratios. Analysis reveals that the strain energy release rate decreases with increasing of E_t/E_0 and S_t/S_0 ratios. The increase of m and p leads also to decrease of strain energy release rate. The loading conditions are characterized by *T/F* and *T/M* ratios. The investigation shows that the strain energy release rate increases with increasing of *T/F* and *T/M* ratios.

The solution derived in the present paper can be applied to calculate the strain energy release rate when analysing lengthwise circular cylindrical cracks in round bars which are functionally graded in the radial direction. The results obtained may be useful in structural design of functionally graded round bars when considering their lengthwise fracture behaviour.

ACKNOWLEDGEMENTS

Rizov gratefully acknowledges the financial support by DAAD for his research stay at the Department of Technical Mechanics, Institute of Mechanics, Otto-von-Guericke-University, Magdeburg, Germany.

REFERENCES

1. Neubrand, A., Rödel, J. (1997), *Gradient materials: An overview of a novel concept,* Zeitschrift für Metallkunde, 88(5): 358-371.
2. Suresh, S., Mortensen, A., Fundamentals of Functionally Graded Materials: Processing and Thermomechanical Behavior of Graded Metals and Metal-Ceramic Composites, IOM Communications Ltd, London, 1998.
3. Hirai, T., Chen, L. (1999), *Recent and prospective development of functionally graded materials in Japan*, Mater Sci. Forum, 308-311(2): 509-514. doi: 10.4028/www.scientific.net/MSF.308-311.509
4. Gasik, M. (2010), *Functionally graded materials: Bulk processing techniques,* Int. J Mater. Prod. Techn. 39(1-2):20-29. doi: 10.1504/IJMPT.2010.034257
5. Hedia, H.S., Aldousari, S.M., Abdellatif, A.K., Fouda, N. (2014), *A new design of cemented stem using functionally graded materials (FGM)*. Biomed. Mater. Eng. 24(3):1575-1588. doi: 10.3233/BME-140962.
6. Yan, W., Ge, W., Smith, J., et al. (2016), *Multi-scale modelling of electron-beam melting of functionally graded materials*. Acta Mater. 115:403-412. doi: 10.1016/j.actamat.2016.06.022
7. Saiyathibrahim, A., Subramaniyan, R., Dhanapl, P. (2016), *Centrifugally cast functionally graded materials - A review*. In: Int. Conf. on Systems, Science, Control, Communication, Eng. and Techn. 2016, 68-73.
8. Erdogan, F. (1995), *Fracture mechanics of functionaly graded materials*, Comppposites Eng. 5(7): 753-770. doi: 10.1016/0961-9526(95)00029-M
9. Tilbrook, M.T., Moon, R.J., Hoffman, M. (2005), *Crack propagation in graded composites*, Composite Sci. & Techn. 65(2): 201-220. doi: 10.1016/j.compscitech.2004.07.004
10. Carpinteri, A., Pugno, N. (2006), *Cracks and re-entrant corners in functionally graded materials*, Eng. Fracture Mech. 73:1279-1291. doi: 10.1016/j.engfracmech.2006.01.008
11. Rizov, V.I. (2018), *Delamination in multi-layered functionally graded beams - An analytical study by using the Ramberg-Osgood equation*, Struct. Integ. & Life, 18(1): 70-76.
12. Rizov, V.I. (2018), *Delamination in nonlinear elastic multi-layered beams of triple graded materials,* Struct. Integ. & Life, 18(3): 163-170.